



Heat transfer from a horizontal bundle of finned tubes to an air fluidized bed  
by Stephen John Priebe

A thesis submitted in partial fulfillment of the requirements for the degree of DOCTOR OF  
PHILOSOPHY in Chemical Engineering  
Montana State University  
© Copyright by Stephen John Priebe (1975)

**Abstract:**

Heat transfer coefficients were measured from a horizontal bundle of finned tubes in an air fluidized bed. Two types of tubes were studied. Discontinuous finned tubes were used to study' fin spacing and heat flux, while spined tubes were used to study spine height, spine material, and number of spines.

Results indicate that fin spacing has little effect when the spacing between fins is greater than 10 particle diameters. At less than 10 diameters, the coefficient begins to fall rapidly up to a point where the spacing is less than two particle diameters. From this point on, the curve falls very slowly, it was also found that the heat transfer coefficient increases slightly as the heat flux is increased.

Results with the spined tubes indicate that the heat transfer coefficient decreased with increasing fin height. Coefficients obtained with copper spines were much higher than those of stainless steel.

There was little difference in the coefficient with larger number of spines. However, the increased area with more fins yields a higher rate of heat transfer. Each type of tube led to a correlation relating heat transfer coefficient to the parameters of interest.

HEAT TRANSFER FROM A HORIZONTAL BUNDLE OF FINNED  
TUBES TO AN AIR FLUIDIZED BED

by

STEPHEN JOHN PRIEBE

A thesis submitted in partial fulfillment  
of the requirements for the degree

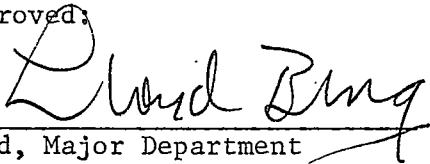
of

DOCTOR OF PHILOSOPHY

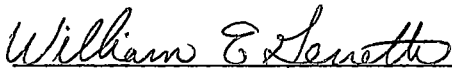
in

Chemical Engineering

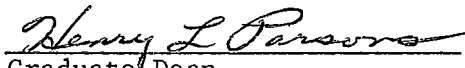
Approved:



Head, Major Department



Chairman, Examining Committee



Graduate Dean

MONTANA STATE UNIVERSITY

Bozeman, Montana

June, 1975

ACKNOWLEDGMENT

The author wishes to thank the staff of the Department of Chemical Engineering at Montana State University for all help give in this research.

Special thanks go to Dr. William Genetti who provided much needed help in most phases of the project.

Finally, the author would like to acknowledge the National Science Foundation who provided the funding for the project. (NSF Grant No. GK-39894)

## TABLE OF CONTENTS

VITA. . . . .	if
ACKNOWLEDGMENT. . . . .	iii
LIST OF FIGURES . . . . .	vi
ABSTRACT. . . . .	viii
I. INTRODUCTION . . . . .	1
II. THEORY AND PREVIOUS RELATED RESEARCH . . . . .	7
MECHANISM OF FLUIDIZATION . . . . .	7
MECHANISM OF HEAT TRANSFER BETWEEN FLUIDIZED BED AND HEAT SURFACE . . . . .	10
PREVIOUS RESEARCH WITH IMMersed TUBES . . . . .	15
III. EXPERIMENTAL PROGRAM . . . . .	20
EXPERIMENTAL EQUIPMENT. . . . .	20
FLUIDIZING COLUMN . . . . .	20
FLUIDIZING SYSTEM . . . . .	22
ELECTRICAL SYSTEM . . . . .	23
EXPERIMENTAL PROCEDURES . . . . .	26
CALIBRATION OF MAIN AIR LINE. . . . .	26
PROCEDURE FOR A TYPICAL RUN . . . . .	26
IV. RESULTS AND DISCUSSION . . . . .	36
PERFORMANCE OF ESCOA FINNED TUBES . . . . .	36
VARIATION OF HEAT TRANSFER COEFFICIENT WITH HEAT FLUX . . . . .	36
EFFECT OF FIN SPACING ON HEAT TRANSFER COEFFICIENT. . . . .	39

## TABLE OF CONTENTS (cont)

	DEVELOPMENT OF THEORETICAL MODEL FOR ESCOA FINNED TUBES.	46
	CORRELATION FOR ESCOA FINNED TUBES . . . . .	52
	PERFORMANCE OF HEATRON SPINE TUBES . . . . .	57
	DEVELOPMENT OF THEORETICAL MODEL FOR HEATRON SPINED TUBES. . . . .	68
	PERFORMANCE OF ALL TUBE BUNDLES USING HEAT TRANSFER COEFFICIENT BASED ON TEMPERATURE DISTRIBUTION. . . . .	78
	CORRELATION OF ALL HEATRON SPINED TUBE BUNDLES . . . . .	83
V.	CALCULATIONS. . . . .	88
	AIR MASS VELOCITY. . . . .	88
	BED TEMPERATURE. . . . .	89
	TUBE TEMPERATURE . . . . .	89
	HEAT INPUT TO EACH TUBE. . . . .	89
	TOTAL TUBE AREA. . . . .	89
	HEAT TRANSFER COEFFICIENT. . . . .	90
	PARTICLE FRACTION. . . . .	90
	AIR VISCOSITY AND THERMAL CONDUCTIVITY . . . . .	91
	PARTICLE REYNOLDS NUMBER . . . . .	91
	PARTICLE NUSSELT NUMBER. . . . .	91
VI.	ERROR ANALYSIS. . . . .	92
VII.	CONCLUSIONS . . . . .	94
VIII.	RECOMMENDATIONS . . . . .	96
IX.	NOMENCLATURE. . . . .	97
X.	BIBLIOGRAPHY. . . . .	99

## LIST OF FIGURES

<u>Figure</u>		<u>Page</u>
1	Regimes of Fluidization . . . . .	3
2	Proposed Mechanism of Heat Transfer . . . . .	14
3	Overall View of Equipment . . . . .	28
4	Details of Fluidizing Column. . . . .	29
5	Details of Cartridge Heater . . . . .	30
6	Details of Finned and Spined Tubes. . . . .	31
7	Details of Heater and Tube Assembly . . . . .	32
8	Photograph of Overall Equipment . . . . .	33
9	Photograph of Finned and Spined Tubes . . . . .	34
10	Photograph of Heater and Tube Assembly. . . . .	35
11	Particle Nusselt Number versus Heat Flux - 6 FPI. . . . .	42
12	Particle Nusselt Number versus Heat Flux - 8 FPI. . . . .	43
13	Particle Nusselt Number versus Heat Flux - 10 FPI . . . . .	44
14	Equivalent Bare Tube Coefficient versus Particle Diameter to Fin Spacing Ratio . . . . .	45
15	Proposed Model of Escoa Fin . . . . .	50
16	Analytical Solution for $Q/\Delta T = f(h)$ . . . . .	51
17	Correlation for All Escoa Finned Tube Bundles . . . . .	56
19	Performance of 1-1/8" OFD Spined Tubes. . . . .	60
20	Performance of 1-1/2" OFD Spined Tubes. . . . .	61
21	Performance of 1-3/4" OFD Spined Tubes. . . . .	62

## LIST OF FIGURES (cont)

<u>Figure</u>		<u>Page</u>
22	Performance of 2" OFD Spined Tubes . . . . .	63
23	Performance of 1-1/8" OFD Spined Tubes . . . . .	64
24	Performance of 1-1/2" OFD Spined Tubes . . . . .	65
25	Performance of 1-3/4" OFD Spined Tubes . . . . .	66
26	Performance of 2" OFD Spined Tubes . . . . .	67
27	Proposed Model for Heatron Spined Tube . . . . .	73
28	Analytical Solution for $Q/\Delta T = f(h)$ Heatron - Copper - 26 SPT. . . . .	74
29	Analytical Solution for $Q/\Delta T = f(h)$ Heatron - Copper - 13 SPT. . . . .	75
30	Analytical Solution for $Q/\Delta T = f(h)$ Heatron - Stainless Steel - 26 SPT . . . . .	76
31	Analytical Solution for $Q/\Delta T = f(h)$ Heatron - Stainless Steel - 13 SPT . . . . .	77
32	Heat Transfer Coefficient Based on Theoretical Model of Spine - 1-1/8" OFD. . . . .	79
33	Heat Transfer Coefficient Based on Theoretical Model of Spine - 1-1/2" OFD. . . . .	80
34	Heat Transfer Coefficient Based on Theoretical Model of Spine - 1-3/4" OFD. . . . .	81
35	Heat Transfer Coefficient Based on Theoretical Model of Spine - 2" OFD. . . . .	82
36	Correlation for All Heatron Spined Tube Bundles. . . . .	87

ABSTRACT.

Heat transfer coefficients were measured from a horizontal bundle of finned tubes in an air fluidized bed. Two types of tubes were studied. Discontinuous finned tubes were used to study fin spacing and heat flux, while spined tubes were used to study spine height, spine material, and number of spines.

Results indicate that fin spacing has little effect when the spacing between fins is greater than 10 particle diameters. At less than 10 diameters, the coefficient begins to fall rapidly up to a point where the spacing is less than two particle diameters. From this point on, the curve falls very slowly. It was also found that the heat transfer coefficient increases slightly as the heat flux is increased.

Results with the spined tubes indicate that the heat transfer coefficient decreased with increasing fin height. Coefficients obtained with copper spines were much higher than those of stainless steel. There was little difference in the coefficient with larger number of spines. However, the increased area with more fins yields a higher rate of heat transfer.

Each type of tube led to a correlation relating heat transfer coefficient to the parameters of interest.



## INTRODUCTION

The fluidized bed has in recent years received considerable attention in a number of industrial applications. However, to enhance use and design, more knowledge of the physical processes occurring in the fluidized bed is needed. The purpose of this thesis is to better understand heat transfer from finned tubes to a fluidized bed.

Basically, a fluidized bed consists of a column, a bed of particles supported on a distributor plate, and a source of fluid to be used as the fluidizing medium. The column may range from a few inches to several feet in diameter. The particles can consist of a wide range of materials, as can the fluidizing medium.

The term fluidization arises from the nature of the bed of particles when sufficient fluid is passed through the bed. At low fluidizing velocities, the fluid, air for example, merely passes through the bed as in a packed bed.

As the velocity is increased, a point is reached when the pressure drop across the bed is equal to the weight of solids in the bed. At this point, the bed expands slightly and acts like a highly viscous fluid. This velocity is called the minimum fluidization velocity. There is very little particle motion at minimum fluidization.

With increased velocity, particulate fluidization may occur. Particulate fluidization occurs primarily in liquid fluidized beds where the density of particles is not very much greater than the liquid. Visually, the bed resembles minimum fluidization, with only a

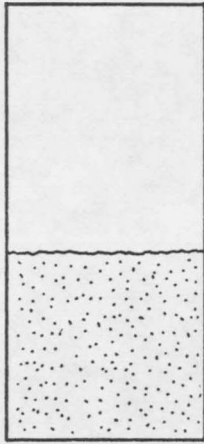
slight increase in particle motion.

In a gas fluidized bed, gas bubbles begin forming almost immediately after the minimum fluidization velocity is exceeded. This bubbling is known as aggregative fluidization. Small bubbles form in the region of the distributor plate and rise through the bed similarly to a boiling fluid. As the bubbles move upward through the bed, they coalesce to form larger bubbles which finally burst at the surface. The size and number of bubbles depend upon the nature of the distributor plate, and bed height. With vigorous bubbling, there is considerable motion with aggregative fluidization.

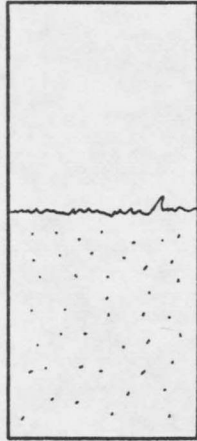
The final regime of fluidization, known as slugging, occurs when slugs of fluid, occupying the entire cross section of the column, pass through the bed. Maximum particle motion occurs during slugging, but physical problems may become important. Particles may be broken down, and smaller particles may be entrained and lost.

Finally, as the velocity is increased beyond slugging, all the particles are entrained and carried out of the column. The various regimes of fluidization are shown schematically in Figure 1.

Industrially, the fluidized bed has been known for quite a long time, but only in the last 40-50 years has it achieved any major importance. At about this time, the petroleum industry discovered that the fluidized bed was very useful in the catalytic cracking unit. This eliminated the need for shutdown and complete regeneration of the catalyst.



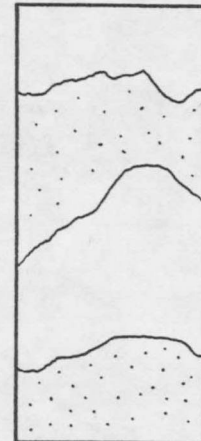
NON-FLUIDIZED



PARTICULATE  
FLUIDIZATION



AGGREGATIVE  
FLUIDIZATION



SLUGGING

FIGURE 1. REGIMES OF FLUIDIZATION

The fluidized bed could be run with a continuous stream of particles being drawn off, regenerated, and recycled to the column.

Since the fluidized catalytic cracker became established, several other widespread applications of the fluidized bed have been made. In desalination of sea water, the sea water is sprayed into a hot bed. The water is evaporated leaving the salt to deposit on the particles.

Another application has been in the treatment of liquid nuclear wastes. Once again, solution is sprayed into a hot bed, allowing the radioactive material to deposit on the particles. The solid particles are then stored underground thus eliminating the bulk and potential leakage of liquid wastes.

In recent years, research has begun in several other areas. One area is fluidized bed combustion of coal for electrical generation plants, where limestone is used as the particulate. A prime advantage of this method is that sulfur in the coal reacts with the limestone thus eliminating  $SO_2$  formation.

Two other recent uses of the fluidized bed have been as a shallow bed cooling tower and as a heat exchanger for geothermal energy.

As shown, there is a wide variety of possible applications for the fluidized bed. However, there are several disadvantages in its use. Listed below are some of the advantages and disadvantages of the fluidized bed.

### Advantages

1. Due to extremely vigorous mixing in a fluidized bed, there are few concentration or thermal gradients. This would be important in many reactions which are strong functions of temperature or concentrations.
2. Continuous recycling of solids is much easier to implement than in a fixed bed.
3. Increased particle activity results in much higher heat transfer coefficients which would make temperature control easier and more efficient.

### Disadvantages

1. Because relative fluid and particle motion is basically co-current, the driving force is not completely favorable, and the fluidized bed acts as a single stage. Multiple beds can overcome this problem, but might run into more expense.
2. Space velocity through the column is limited, because the bed fluidizes only in a relatively narrow range of velocities.
3. Particle degradation and elutriation may cause severe catalyst losses.
4. In some systems, particle agglomeration may plug a fluidized bed to the point where proper operation is not possible.

This shows that while a fluidized bed might be very useful

in some cases, each application must be studied with care.

In most of the applications above, heat must be transferred to or from the fluidized bed. Originally this heat transfer was accomplished through the walls of the column. However, this severely limits the available surface area for heat transfer. To overcome this problem, either horizontal or vertical tubes are placed in the bed.

Since heat transfer coefficients have been shown to be much greater in a fluidized bed than in a similar column without the bed of particles, it is necessary to learn as much as possible about the heat transfer from immersed tubes. In many other heat transfer systems, finned surfaces have been shown to greatly increase the heat transfer. It seems probable then that finned tubes might also enhance heat transfer in a fluidized bed, thereby reducing the total number of tubes.

The purpose of this research was to study the effect of fin spacing on discontinuous finned tubes, (a type of tube similar to those used by Bartel [1]), on heat transfer coefficients. In addition, spined tubes were studied. The effects of fin height and fin material on the heat transfer coefficients were determined.

## THEORY AND PREVIOUS RELATED RESEARCH.

### Mechanism of Fluidization

To better understand the process of heat transfer in a fluidized bed, some knowledge of the mechanism of fluidization is helpful. To simplify the process, a single gas bubble will be considered first.

A model proposed by Davidson and Harrison (3) contains three major conditions:

1. The gas bubble is spherical and particle free.
2. The particles around the bubble move as an inviscid fluid.
3. In the bulk phase, the gas flows incompressibly through the bed.

In addition to these three conditions, they also assumed that the pressure gradient far from the bubble is unaffected by the bubble passage, and that the pressure in the bubble is constant.

This model has been shown to be mostly correct with only minor changes, such as the shape of the bubble. Visual observations (14) have shown the bubble to have a concave bottom into which flows gas and some particles.

Extending this model to include multiple bubble formation and bubble interactions leads to a model proposed by Kunii and Levenspiel (7).

1. A wake of particles and gas follows each bubble in its upward travel.
2. Solids in the wake are constantly being renewed and move

upward at a velocity,  $U_b$ . At the top of the bed, the solids begin to move downward at a velocity,  $U_s$ .

3. The following relation between the bulk phase velocity,  $U_e$ , and the downward solids was proposed:

$$U_e = \frac{U_{mf}}{\epsilon_{mf}} - U_s$$

where,

$U_{mf}$  = velocity of fluid at minimum fluidization

$\epsilon_{mf}$  = void fraction at minimum fluidization

This model has been shown to do a reasonably good job describing the action of the fluidized bed. However, it must be remembered that this model applies only to aggregative fluidization.

A study was conducted by Hager and Thomson (5), on the effect of immersed tubes on bubbles traveling through a fluidized bed. Visual and x-ray techniques were used to study the motion of bubbles around bare and finned tubes.

With horizontal bare tubes, about 50 percent of the bubbles divided when passing over the tube. These bubbles quickly coalesced above the tube. The remainder of the bubbles were diverted around the tube.

With finned tubes, the action was somewhat different. Here, most bubbles were either diverted around the tube, or entered the fin



structure, eventually emerging at the top of the tube. When a bubble did divide, the two halves passed around the outside of the fin structure. When this occurred, there was little particle motion between the fins.

Mechanism of Heat Transfer Between Fluidized Bed and Heat Surface

When studies showed that heat transfer coefficients were much higher in fluidized systems than in empty columns, interest was generated in developing some idea as to the reason for the increase. Several explanations have been made and most of them probably contribute to the overall picture.

A number of people, including Leva, et al. (9) and Levenspiel and Watson (10), proposed a scouring mechanism. In this model, the normal boundary layer on the heat transfer surface is partially scrubbed away by the action of the particles. When the boundary layer is thinned, the resistance is reduced thereby increasing heat transfer. Levenspiel developed a relation to describe the effective film thickness in both laminar and turbulent flow conditions. The relation describes the scouring and the growth rate.

A different model was proposed by Mickley and Fairbanks (11). According to this model, packets of particles were viewed to be the heat transfer agent. These packets were said to move from the bulk phase to the heater surface. After remaining at the surface only a short time, the packet returned to the bulk phase where the packet was dispersed.

Mickley, et al. found the heat transfer coefficient to be a function of the quiescent bed thermal conductivity as follows:

$$h = \sqrt{k_m \rho_m c S}$$

where

$k_m$  = thermal conductivity of the packet, BTU/hr-ft-°F

$\rho_m$  = density of packet, lb<sub>m</sub>/ft<sup>3</sup>

$c$  = heat capacity of packet, BTU/lb<sub>m</sub>-°F

$S$  = stirring factor

The stirring factor is basically a function of the hydrodynamics of the system, but is not understood well.

About ten years ago, this model was modified by Ziegler, Koppel, and Brazelton (16). This new model was then extended by Genetti and Knudsen (4). Under this new model, a single particle rather than a packet moves from the bulk phase to near the heater surface. The fluid near the surface is assumed to be at the temperature of the heater. The particle is heated by convection from the hot fluid and then returns to the bulk phase where the heat is dissipated.

The hot gas near the surface is assumed to be a constant temperature, and the contact between the surface and the particle is neglected. The particles are packed rectangularly, and a gamma function is assumed for the residence time of the particles.

With these assumptions, the following expression for the particle Nusselt number was developed.

$$Nu_p = \frac{7.2}{\left[ 1 + \frac{.6 k_{air} \bar{t}}{\rho_s C_{p_s} D_p^2} \right]^2}$$

where,

$Nu_p = hD_p / k_{air} =$  particle Nusselt number

$k_{air} =$  thermal conductivity of air, BTU/hr-ft-°F

$\bar{t} =$  mean residence time of particles, hr

$\rho_s =$  particle solids density, lb<sub>m</sub>/ft<sup>3</sup>

$C_{p_s} =$  heat capacity of particles, BTU/lb<sub>m</sub>-°F

$D_p =$  particle diameter, ft

$h =$  heat transfer coefficient, BTU/hrft<sup>2</sup>-°F

As can be seen from this expression, the particle Nusselt number is not a function of the thermal conductivity of the particles.

Genetti and Knudsen proposed that the constant, 7.2, be replaced by a function of the square root of the particle fraction,  $(1-\epsilon)^{0.5}$ .

It has been proposed that the arithmetic average of the surface temperature and the bulk temperature be used as the film temperature. This model, shown in Figure 2, will be used to correlate the results of this research.

To check the validity of this model, Ziegler and Brazelton (15)

conducted an experiment with both heat and mass transfer. The system they used was an absorbent clay sphere saturated with water.

This sphere was suspended in an empty column and then in a fluidized bed. The fluidized bed particles were non-absorbent, so that under the assumptions of the model, heat transfer rates should increase much more than mass transfer rates.

Results of the experiments showed an increase of 1.5 to 2 times for the mass transfer whereas heat transfer increased 10 to 20 fold. From these results, they concluded that 85-90 percent of the heat transfer can be accounted for by a particle mode of transfer.

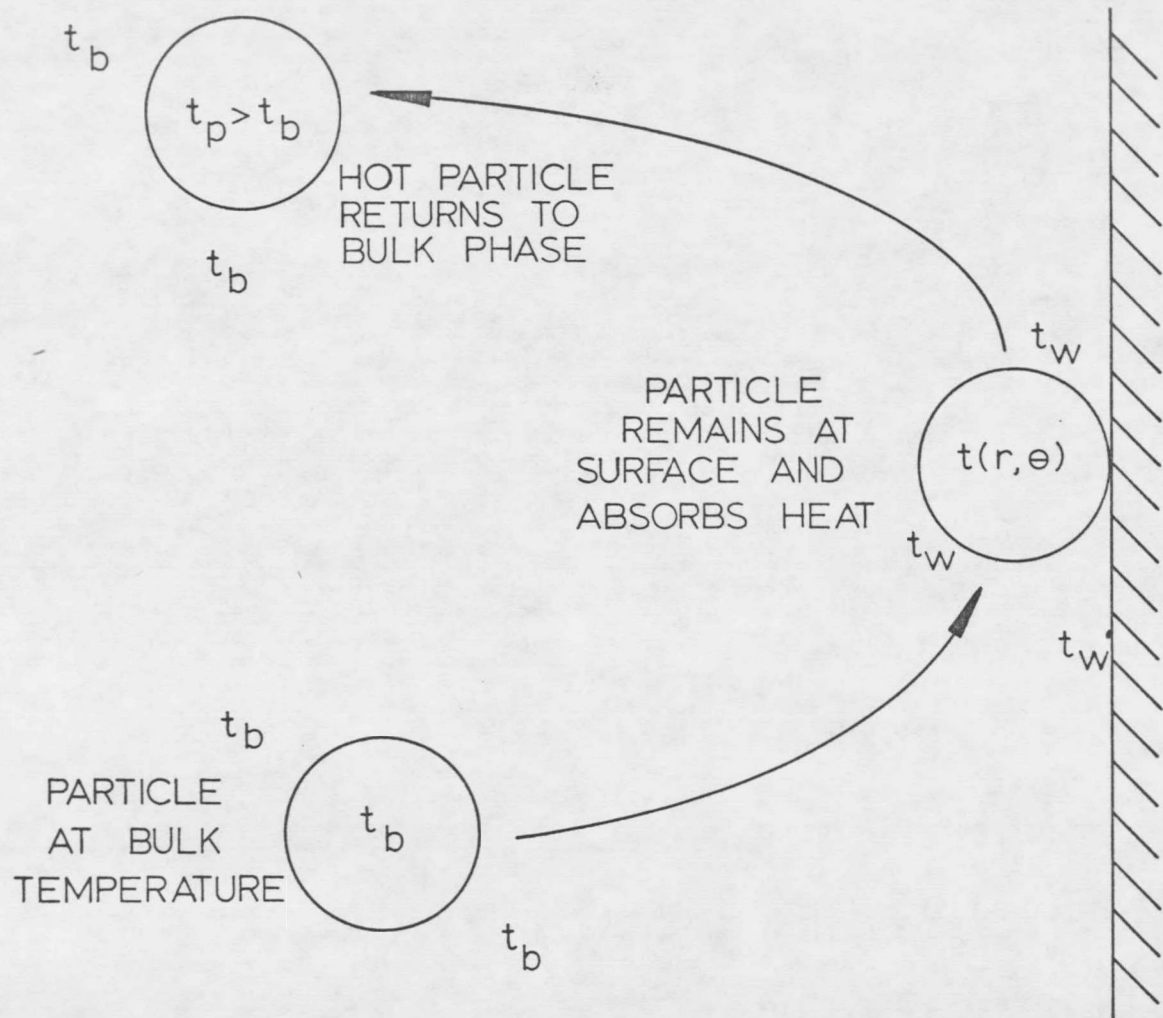


FIGURE 2. PROPOSED MECHANISM OF HEAT TRANSFER

Previous Research with Immersed Tubes

Since immersing tubes in a fluidized bed can greatly increase the area for heat transfer, it is important to learn as much as possible about what parameters affect heat transfer from the tubes to a fluidized bed. The end result should be a design equation that can be used in a large number of applications.

In this respect, several people have investigated heat transfer from tubes in a fluidized bed. Originally, this was done with horizontal or vertical bare tubes with advantages to each.

On a vertical tube, the particles tend to remain in contact with the heater longer thus receiving more heat. However, the particle transfer is much slower than with horizontal tubes. In a study conducted by Genetti, Schmall and Grimmitt (14), the tube orientation angle was studied. Their results showed that the heat transfer coefficient passed through a minimum as the tube was moved from a horizontal to vertical position. The angle at the minimum was different for bare and finned tubes. Since a column was available which used horizontal tubes, this is what was used for the present research.

An important study by Vreedenberg (13) resulted in a correlation for a single horizontal bare tube. This correlation took the following form:

$$Nu_t = 420 Pr^{0.33} \left( \frac{GD_{p,u}}{D_p^3 \rho_s \rho_g} \right)^{0.33}$$

where,

$Nu_t = h \cdot D_t / k =$  Nusselt number based on tube diameter

Pr = Prandtl number of fluidizing air

k = thermal conductivity of air, BTU/hrft-°F

G = air mass velocity,  $lb_m/hr-ft^2$

$D_t$  = tube diameter, ft.

$\rho_s$  = apparent particle density,  $lb_m/ft^3$

$\rho_g$  = density of air,  $lb_m/ft^3$

g = gravitational constant,  $ft^2/hr$

The fluid properties were evaluated at the bed temperature.

In research conducted by Petrie, Freeby, and Buckham (12) bundles of bare and finned tubes were studied. The tubes were heated either electrically or with steam condensing on the inside.

Their bare tube data correlated into the following relation:

$$Nu_t = 14 \left( \frac{G}{G_{mf}} \right)^{0.33} (Pr)^{0.33} \left( \frac{D_t}{D_p} \right)^{0.667}$$

where,

$G_{mf}$  = minimum fluidization velocity,  $lb_m/hr-ft^2$

It can be noted that in both the correlation by Vreedenberg, and that by Petrie, et al. the Nusselt number is dependent upon both the air mass velocity and particle diameter. Both investigations indicated



that the heat transfer coefficient increases with air mass velocity, but decreases with particle diameter.

Petrie, et al, indicated that for tube bundles, the spacing between tubes had no effect when the tube separation was, over 43 particle diameters indicating that the tubes were acting independently.

The dependence of the heat transfer coefficient on air mass velocity has been well established. Rather than always being monotonically increasing, as indicated by the above correlations, the coefficient may pass through a maximum at some air velocity. The existence and location of this maximum depends on the diameter and density of the particles.

Studies have shown (2,6) that a stagnant cap exists on top of a horizontal tube, where heat transfer is up to seven times smaller than at the sides. The stagnant cap is constantly being regenerated, with the rate dependent on air velocity.

Research with finned tubes has been very limited until recently. The work of Petrie, et al. (13), using tubes of 5 and 11 fins per inch, indicated that, although the heat transfer coefficient decreased with more fins, the increased area actually caused greater heat transfer rates.

Another study, using discontinuously-finned tubes, was conducted by Bartel (1). In his research, Bartel looked at several parameters including fin height, particle size, tube to tube spacing, and air

mass velocity.

His results showed that heat transfer coefficients decreased with fin height, but this effect was more than compensated for by the additional area. Coefficients were also found to be affected by tube spacing with the effect being smaller with longer fins. He found the effect to be noticeable to a spacing of about 100 particle diameters.

Bartel correlated his results into a form similar to that of Genetti and Knudsen (4). In the correlation, the particle Nusselt number was related to the four parameters studied.

$$Nu_p = \frac{10(1-\epsilon) \left[ 1 - \frac{0.027 + 4.3L^{1.5}}{p(1.12 + 3.2L^{0.6})} \right]}{\left[ 1 + \frac{0.00102 + 0.047L^{0.80}}{Re_p (0.33 + 0.40L^{9.33}) D_p (1.23 + 0.57L^{0.25})} \right]^2}$$

where,

L = fin height, inches

P = distance between tube centers, inches

D<sub>p</sub> = particle diameter, inches

Re<sub>p</sub> = D<sub>p</sub>G/μ = particle Reynolds number

This expression was found to fit all the data within  $\pm 15\%$ .

The model Bartel used to describe the fins was not tested, as only one fin material, carbon steel, was used.

The present study uses the same column as used by Bartel, but

involves copper and stainless steel spined tube bundles. Using two materials allows a check on the mathematical model of heat conduction in the spine.

## EXPERIMENTAL PROGRAM

### EXPERIMENTAL EQUIPMENT

As mentioned earlier, the basic equipment used in this research was already available, so only minor modifications were required. Most of the changes were made to make the system either more efficient or to improve safety. The discussion of the equipment will be divided into three sections: 1) the column, 2) the fluidizing system, and 3) the electrical system.

An overall view of the equipment is shown in Figure 3. It shows the relationship between various parts of the system.

### Fluidizing Column

Figure 4 shows a detailed view of the column used in this study. The column was constructed of 3/4" clear plexiglass and had a rectangular cross section (14" x 6.5"). The column was clear to allow visual observation of the bed when fluidized. In this way, such things as channeling and slugging could be seen. It was also easier to see that the heaters and tubes were properly in place.

A rectangular cross section was chosen so that all the tubes would be in the same relative position to the walls. Also, it was easier to fabricate this type of column.

The column was about 8 feet tall, with about 1.5 feet below the distributor plate. This allowed sufficient room above the bed for the bed to act freely. The space below the bed allowed for some smoothing

of air flow before entering the particle bed.

Two micarta plates (laminated canvas) were used to hold the heater-tube assemblies. In one plate, holes were drilled completely through and fitted with Swagelock fittings, through which the heaters extended. The other plate had partial holes drilled to hold the end of the heaters. This held the tubes firmly in place. The two plates were removable and held in place by "trunk lid" type clamps.

The top of the column was removable so that particles could be poured in. A large rectangular hole was cut in the top and covered with 200 mesh stainless steel wire cloth. This hole, in addition to four smaller holes located on the sides at the top, allowed the air to leave the column. Previously, five small holes had been cut in the top rather than the larger rectangular hole. However, it was found that the small holes plugged with particles at higher flow rates, thus lowering the velocity.

To ease emptying and cleaning the column, a particle drain and two vacuum ports were included. The drain was a 1" diameter pipe extending through the bottom of the column, with a valve in the line. The two vacuum ports were 3" circular holes cut in either side of the column just above the distributor plate. Each hole was fitted with a removable plug.

The distributor plate consisted of two layers of 200 mesh wire cloth sandwiched between two perforated steel plates. This proved to

provide sufficient pressure drop for uniform fluidization, though at low velocities some channeling occurred.

Located in the entrance section, below the distributor plate, were two rows of 3/4" horizontal tubes. These tubes were intended to straighten the air flow as it entered the column.

The column was supported by four angle irons with wooden blocks wedged between the column and the supports. The entire assembly was then bolted to the floor.

#### Fluidizing System

Air, used as the fluidizing medium, was supplied to the column by a Sutorbilt air blower driven by a 7-1/2 hp motor. A 3.5 inch schedule 80 pipe served as the main air line. A similar pipe was used for a bypass line. Two gate valves, one in each line, controlled the air flow. In this study, the main air line valve was left fully open to obtain the necessary velocities.

An orifice in the main line was used to measure flow rates. The pressure drop across the orifice was measured with a water manometer. The orifice had a 1.5 inch diameter opening, and vena contracta taps. For small pressure drops, a micromanometer was also available.

At higher velocities, when fluidization becomes vigorous, the pressure drop across the orifice fluctuates up to 1 to 2 inches of water making accurate readings difficult.

Back pressure from the column is measured with a Duragauge pressure gauge. The tap for this line was located between the orifice and the distributor plate.

The bed material was spherical glass beads of two diameters; 0.011 and 0.0505 inch. The smaller glass beads, manufactured by 3M, had a density of 156 lb/ft<sup>3</sup> while the larger beads, manufactured by Microbeads, Inc., had a density of 198 lb/ft<sup>3</sup>. A bed depth of 23 inches was used for all runs.

To measure the void fraction in the fluidized bed, the pressure drop across the bed was measured with another water manometer. Here, fluctuations in pressure drop were even more severe than with the orifice manometer. Fluctuations of up to 50% of the mean value have occurred, but since the void fraction does not change a great deal, a reasonable good value can be found.

Two mufflers were included; one on the main air line, and one on the bypass line. In addition, the motor and blower were encased in a sound proof box. This helped to cut down the noise of the system.

#### Electrical System

The electrical system consisted of the heater and tube assemblies and the thermocouple system. In this research Calrod Firerod cartridge heaters were used. As shown in Figure 5, there is a 6.5 inch heated

section with a 0.4 inch insulated section on one end. The other end, 2.5 inches long, is also insulated and contains the two leads from the heater. A 1/8" diameter longitudinal hole is drilled through the lead end of the heater. The thermocouple wire from the tube was passed through this hole and hence out of the column.

The leads from the heaters were connected through fuses to seven parallel toggle switches. From these switches, the line ran through a Simpson model 390 wattmeter and then to a Fenwall model 524 high temperature limit protector. This instrument is essentially a cutoff relay to avoid problems of overheating in the bed. A thermocouple in the bed acted as the sensing device for the instrument.

Finally, the line passed through a rheostat and a variac to the line source. Both 120 and 240 volt line sources were used.

Two types of finned tubes were used in this work. The two types are shown schematically in Figure 6, and photographs are shown in Figures 9 - 10. All the tubes were 6.5 inches long and 0.5 inch inside diameter.

The first type of tube, manufactured by Escoa Fintube, had three fin spacings, 6, 8 and 10 fins per inch and were made of carbon steel. The fins had a rectangular cross section. The fins on these tubes were wrapped around and then spot welded to the tube.

The second type of tube, manufactured by Heatron, Inc., is a spined tube. The shape of these fins will be discussed in detail



later, but they are nearly triangular in cross section. These tubes came with several spine heights (ranging from 0.34 to 0.76 inch), two numbers of spines per turn (13 and 26), and two materials (copper and stainless steel). The spines on the tubes were machined directly from the surface of the tubes.

A total of ten thermocouples, not including the one for the high limit temperature protector, were used. One thermocouple was soldered to the surface at the center of each of the seven tubes in the bundle. The wire was then passed through the heater as explained before.

Three thermocouples were located in the bed: one above, one below, and one in the middle of the tube bundle. The bed thermocouples were threaded into pieces of 1/8" copper tubing to protect them from the action of the bed. The end of each tube was covered with wire cloth.

In this manner, the thermocouples measured the temperature of the air rather than the particle temperature. An unprotected thermocouple indicated that the particle temperature was only about 3°F higher than the air.

The thermocouple leads were connected through a switching box to a Honeywell-Brown chart recorder. The recorder replaced a potentiometer previously used, because a fluctuation in temperature of 5-10°F made using the potentiometer very difficult. A history of the temperature was needed to obtain a reliable average.

## EXPERIMENTAL PROCEDURE

### Calibration of Main Air Line

Since some minor changes had been made in the equipment, it was decided to recheck the calibration of the main air line. In the previous use of the column, it was felt since the orifice manometer level fluctuated, some standardizing method should be employed. To do this, the main air line was left fully open, and the bypass valve was marked to show how far open it was. Then by calibrating the markings to the air velocities desired, the flow rates were assumed to be more reproducible.

For this research, it was observed that deviations did occur with this method. Therefore, the pressure drop was measured directly from the manometer for each run.

### Procedure for a Typical Run

The basic procedure was the same for all runs. A set of tubes was selected, and the thermocouples were installed. Before inserting the heater into the tube, the heater was coated with copper anti-seize compound to insure uniform thermal contact.

The heater was then inserted into the tube and the assembly was placed into the micarta plate. The micarta plate was fastened to the column and the ends of the heaters positioned in the holes in the opposite side. The tubes were rotated so that all thermocouples were

on top of the tube.

The column was sealed, to prevent air and particle leakage, using a silicone latex sealant. Particles of the proper size were poured in the top of the column to a static bed height of 23 inches.

The top of the column was clamped on and the blower was turned on. After the flowrate was set, the column was allowed to reach steady state. Steady state for the first run took about four hours, and for each successive run, about 1-1/2 hours. To obtain the maximum number of runs in a day, the column was run overnight.

To change particles, the particles were drained out through the particle drain. The remaining particles were cleaned out through the vacuum ports. New particles could then be placed in the column.

To change tubes, the particles were drained out and the micarta plate was removed. The new bundle of tubes was then set as before.

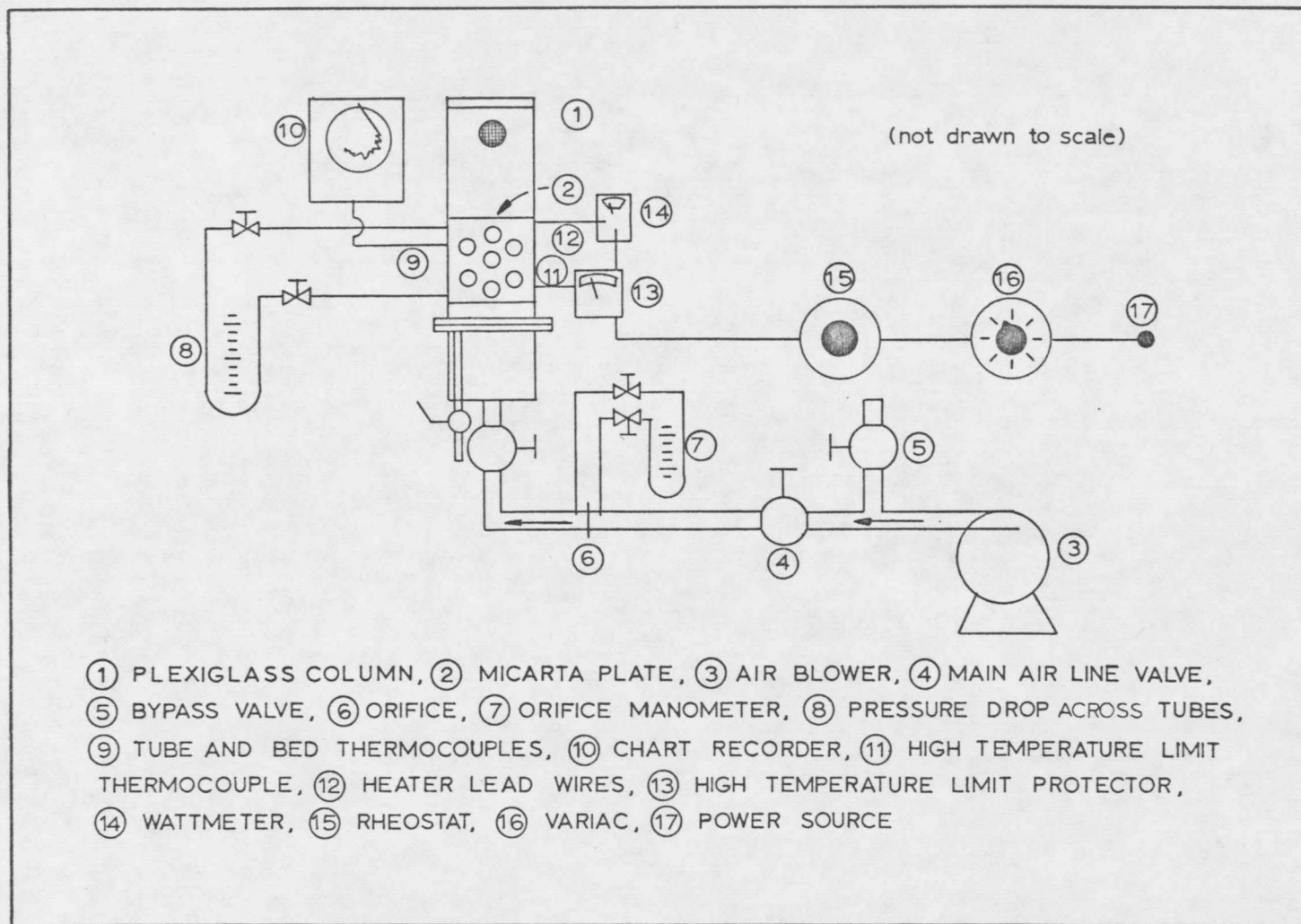


FIGURE 3. OVERALL VIEW OF EQUIPMENT

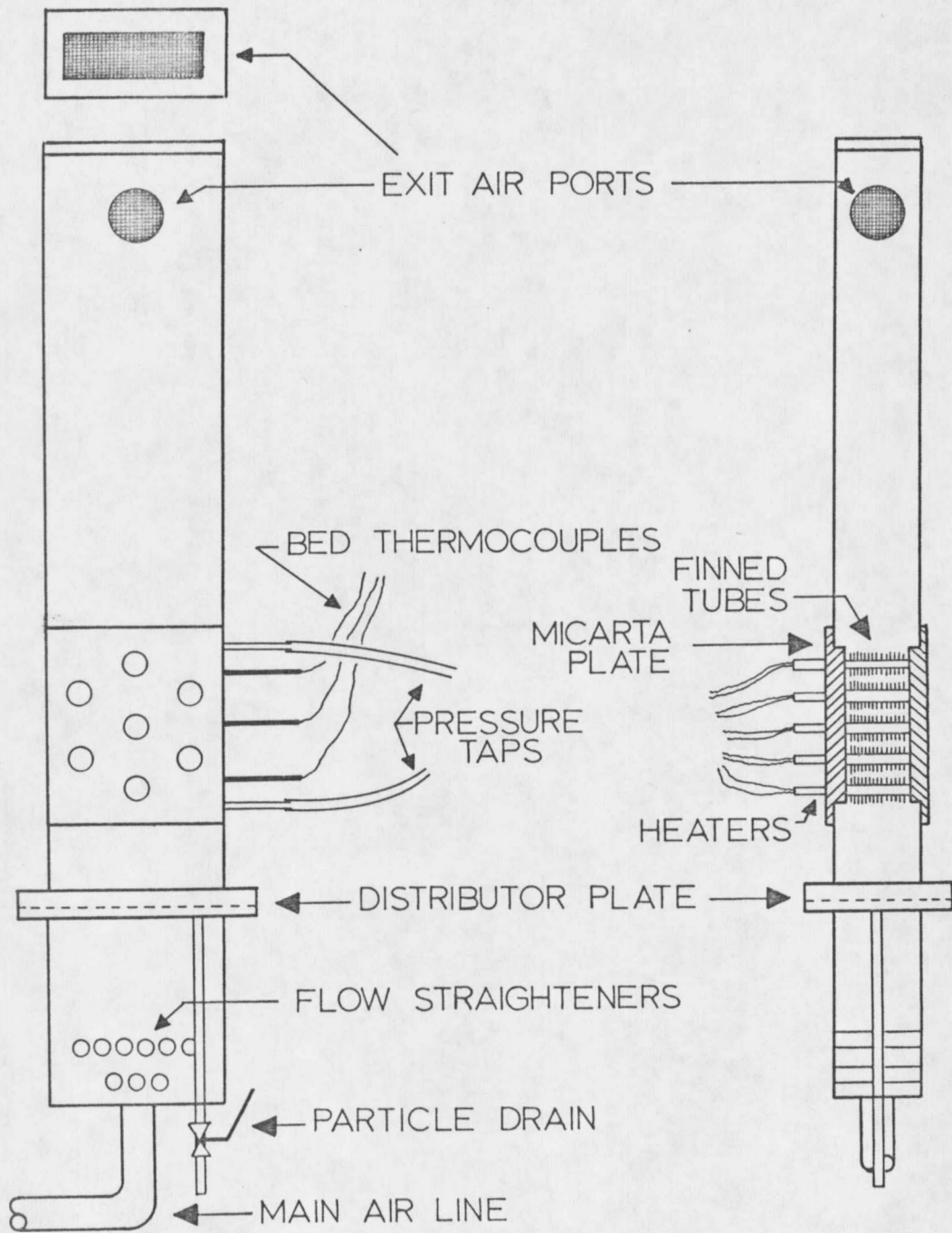


FIGURE 4. DETAILS OF FLUIDIZING COLUMN

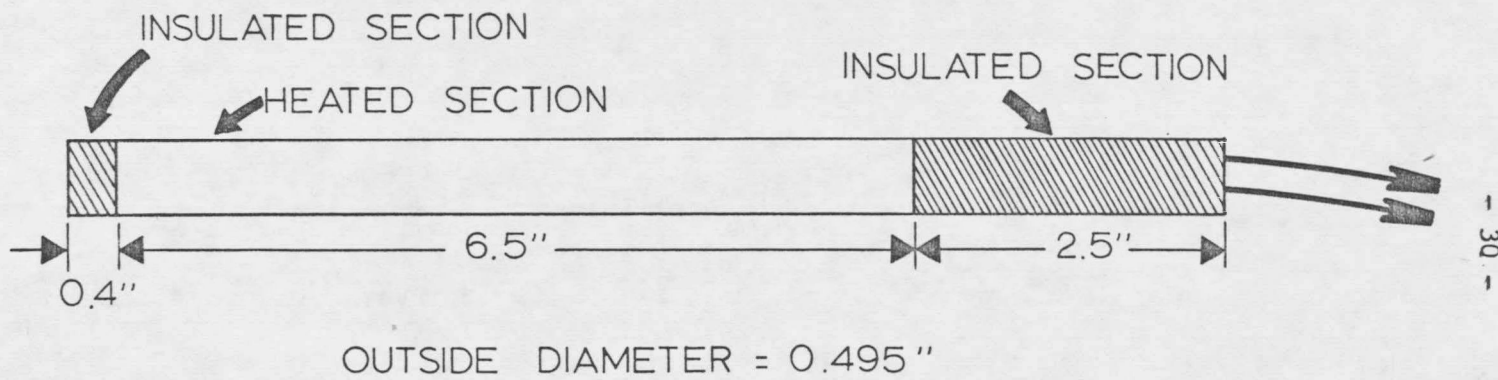
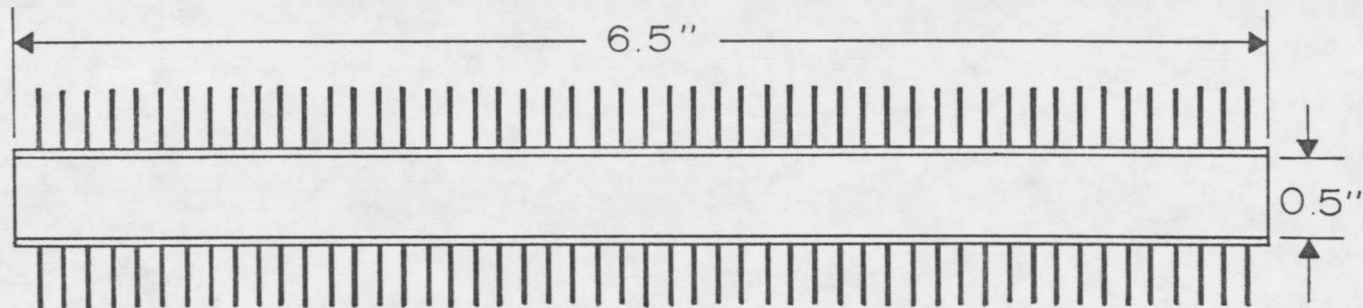


FIGURE 5. DETAILS OF CARTRIDGE HEATER



ESCOA  
FINTUBE



HEATRON  
THERMEK

FIGURE 6. DETAILS OF FINNED AND SPINED TUBES

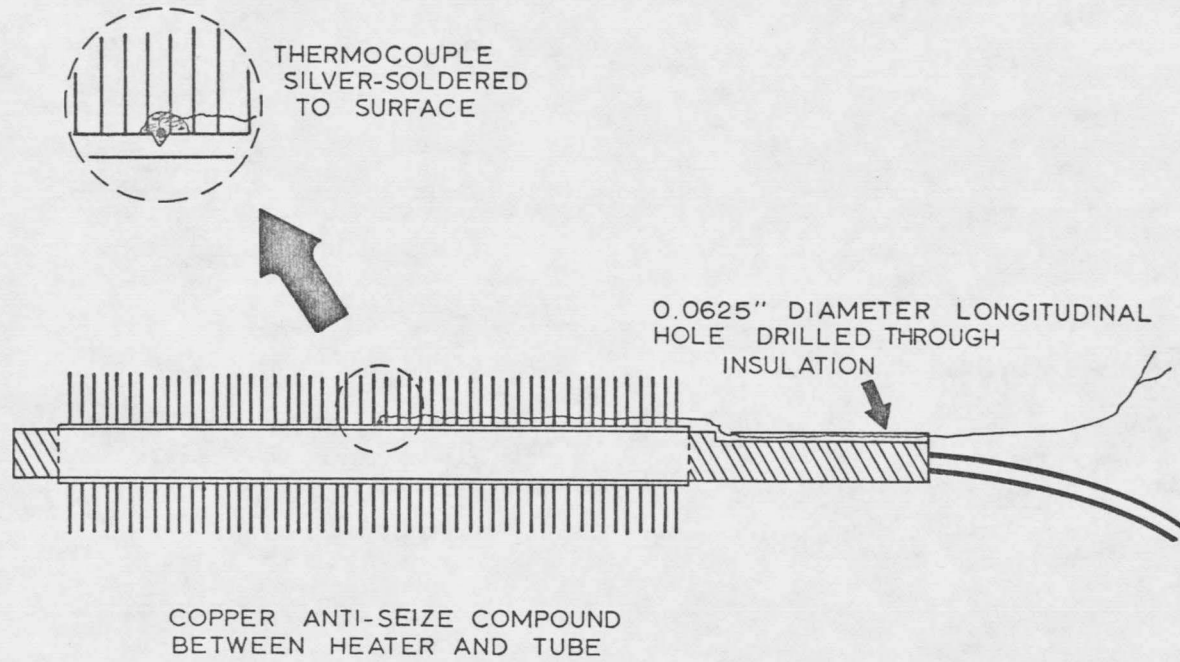


FIGURE 7. DETAILS OF HEATER AND TUBE ASSEMBLY



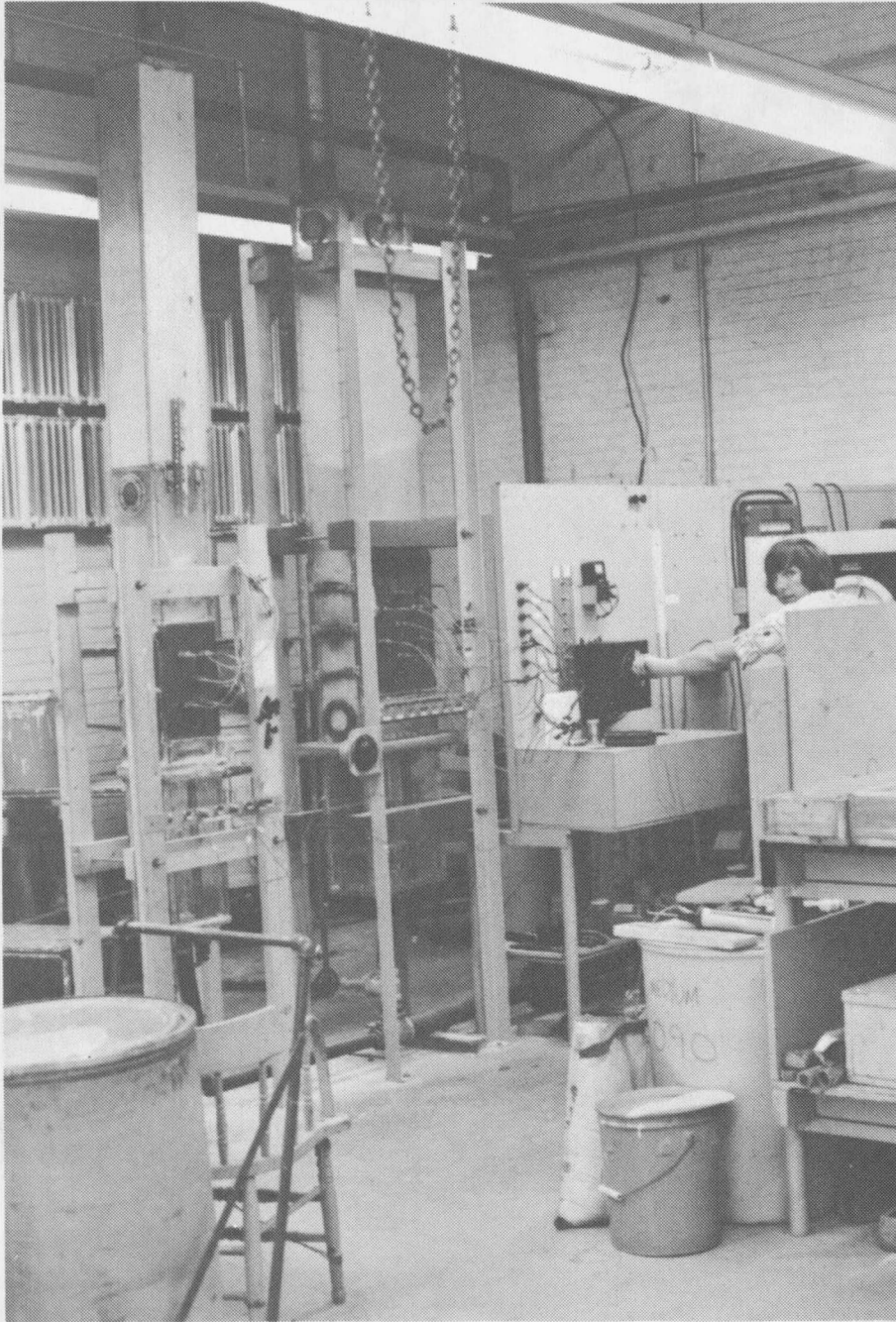


FIGURE 8. PHOTOGRAPH OF OVERALL EQUIPMENT

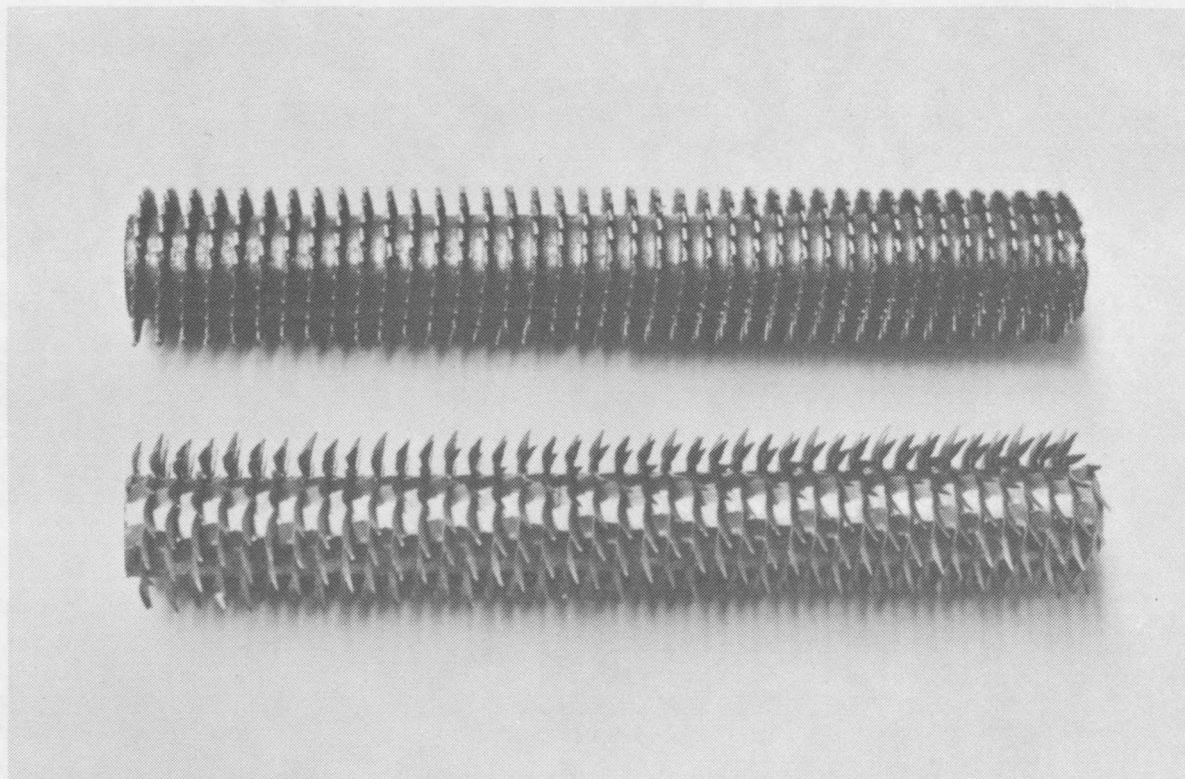
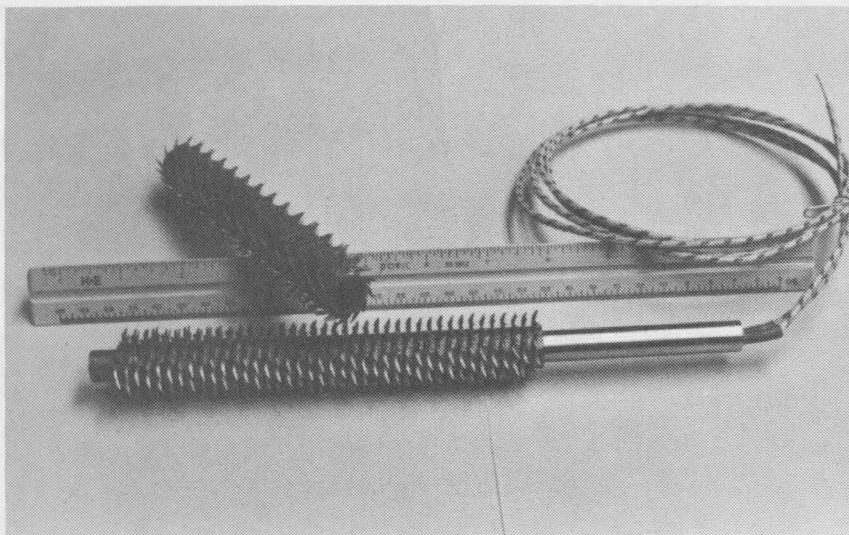


FIGURE 9. PHOTOGRAPH OF ESCOA TUBE (above) AND HEATRON TUBE (below)



HEATRON SPINED TUBE ASSEMBLY

ESCOA FINNED TUBE ASSEMBLY

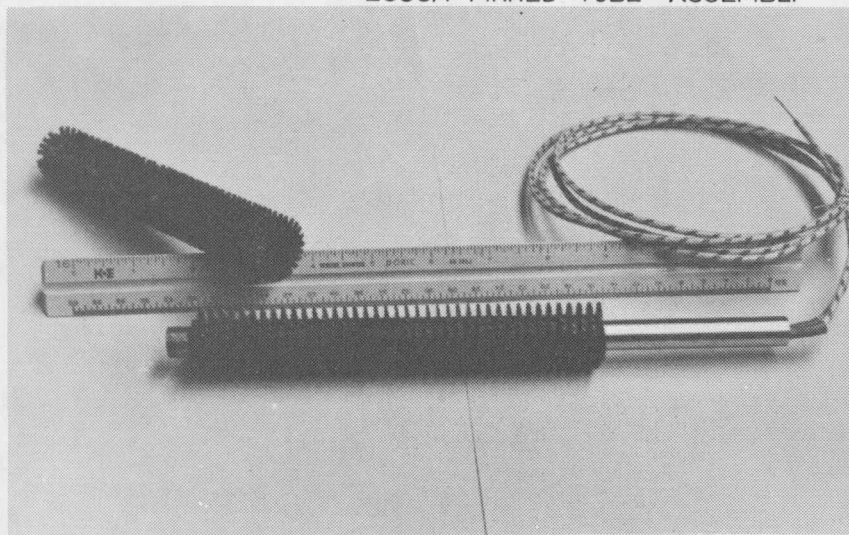


FIGURE 10. PHOTOGRAPH OF HEATER AND TUBE ASSEMBLIES

## RESULTS AND DISCUSSION

This research was divided into two primary parts; one part was conducted using the Escoa finned tubes and the other part using the Heatron spined tubes. The Escoa finned tubes were used to study the effects of fin spacing and heat flux on heat transfer coefficients. The Heatron spined tubes were used to determine the effects of spine height, number of spines, and tube material.

### PERFORMANCE OF ESCOA FINNED TUBES

Three different bundles of Escoa finned tubes were used in this research. The important parameters studied were particle diameter to fin spacing ratio, heat flux and air mass velocity.

### Variation of Heat Transfer Coefficient With Heat Flux -

While operating the equipment in this research, it was observed that fluctuations occurred in the heat input to the column. Therefore, as a preliminary study, it was decided to determine the effect, if any, this variation might have on the heat transfer coefficients.

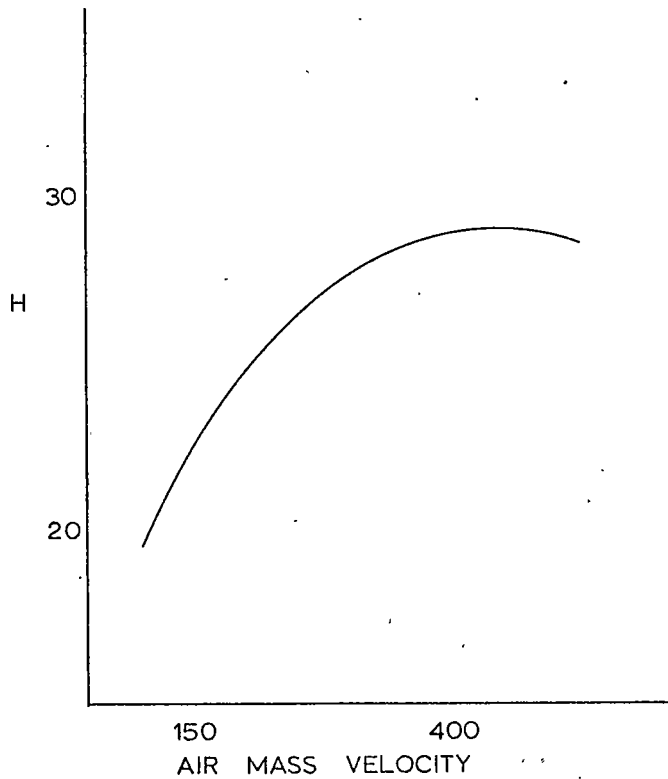
The heat flux to the tube was varied using a variac. The minimum heat flux used was limited by the temperature difference; as the temperature difference gets too small, about 10°F, errors in the heat transfer coefficient can become large. This study was performed with each of the Escoa fin tube spacings.

The results of this study are plotted in Figures 11 - 13 in the form of particle Nusselt number versus heat flux. The Nusselt number

used here is calculated using a heat transfer coefficient based on a theoretical model for heat transfer in the fin.

Briefly, this model accounts for the temperature distribution in the fin, and will be discussed in detail on page 46.

The third parameter in the plots is the air mass velocity. In all three graphs, there is a tendency for more scatter in the data at lower velocities. This is due to the dependence of heat transfer



coefficient on air mass velocity. As shown above, the curve is much steeper at low velocities than at higher velocities. Since it was not possible to control the flow rate exactly, there were small variations in the velocities. Therefore, since the curve is steeper, there was more scatter at low velocities.

From the plots of Nusselt number versus heat flux, it can be seen that there is a positive dependency of heat transfer coefficient on heat flux. The effect is relatively small, being about 10% over the entire range of heat fluxes studied.

A qualitative explanation of the results can be made, however, it is very difficult to verify the explanation experimentally. In the region of the heater surface, there is a thermal boundary layer which is assumed to be only a few particle diameters thick (17). The edge of the boundary is defined as being the point at which the temperature is some percentage, (say 95%) of the bulk temperature.

According to a particle mode of heat transfer, the heat transfer coefficient will be dependent upon the number of particles in the hottest region near the heater. Then, when the heat flux is increased, the temperature difference increases thereby increasing the thickness of the boundary layer. With a thicker boundary layer, more particles can get into the hotter region, so the heat transfer coefficient will increase.

In some cases, it was also observed that the slope of the plot

increased with increased air mass velocity. This is probably because the boundary layer is thicker at lower velocities. Therefore, at low velocities, an increase in boundary layer thickness due to higher heat flux will cause a smaller relative increase in the number of particles entering the hot region. This will result in a smaller slope with low velocity than at high velocity.

Since most normal fluctuations in operating heat input were less than 3 percent, this should result in less than 2 percent variation in heat transfer coefficient. Since this is rather small compared to the possible experimental error, it has been neglected for the remainder of this study.

#### Effect of Fin Spacing on Heat Transfer Coefficient -

It has been suggested qualitatively that there should be some effect on heat transfer coefficient when the spacing between fins gets small relative to the particle diameter. However, aside from the very limited study by Petrie, et al. (12), there has been very little quantitative work done with fin spacing.

The present study investigated three fin spacings and two particle diameters. This gave nearly an order of magnitude range for the ratio of particle diameter to fin spacing.

Since the two particles were of different densities, an attempt was made to run both particles at dynamic similarity. For this system

it was felt that dynamic similarity could be approximated by using the same ratio of fluidizing velocity to minimum fluidization velocity. Limitations of the equipment with respect to the large particles meant that only one mass velocity could be used. This gave a value of  $G/G_{mf} = 1.3$ .

Silica sand was used in addition to the spherical glass beads. The sand had an average diameter of 0.011 inch, the same as the small glass beads. The sand was used to check the effect of an irregularly shaped particle.

The heat transfer coefficient used to plot the data was corrected to account for the differences in total surface area between the three fin spacings. This was done by multiplying the heat transfer coefficient, based on the model, by a ratio of total area to bare tube area. This will then put all the coefficients on the same bare tube area basis.

The corrected heat transfer coefficient is plotted against the ratio of particle diameter to spacing between fins ( $D_p/S$ ), in Figure 14. At  $D_p/S < 0.1$  there is little effect on heat transfer coefficient, implying that the particles are free to move in and out between the fins.

When the fin spacing is less than ten times the particle diameter, the curve begins to fall off sharply. This is probably because the particles are becoming hindered. The particles can no longer move



freely around the fins.

As the particle diameter approaches the fin spacing, the curve begins to level off again. At this point, the heat transfer coefficient is about one half the value when  $D_p/S < 0.1$ . Large parts of the fin are not used because few particles can fit between the fins.

Finally, a point is reached where the particle diameter is greater than the space between the fins. No particles could enter between the fins, this eliminating nearly all the fin area.

In determining the actual heat transfer rates from the tubes, there will be a trade off between the lower heat transfer coefficient with more fins, and the increased area.

To relate this trade off mathematically, it will be necessary to develop a correlation relating the heat transfer coefficient to the ratio  $D_p/S$  and to the particle Reynold's number. This correlation will be developed in the next section.





































































































































